# Brain system for mental orientation in space, time, and person

Michael Peer[a,b,1], Roy Salomon[c,d,1], Ilan Goldberg[b,e], Olaf Blanke[c,d], and Shahar Arzy[a,b,2]

[a]Department of Neurology, Hadassah Hebrew University Medical Center, Jerusalem 91220, Israel; [b]Neuropsychiatry Laboratory, Faculty of Medicine, Hadassah Hebrew University Medical School, Jerusalem 91220, Israel; [c]Center for Neuroprosthetics, School of Life Sciences, École Polytechnique Fédérale de Lausanne, Campus Biotech, 1202 Geneva, Switzerland; [d]Laboratory of Cognitive Neuroscience, Brain Mind Institute, École Polytechnique Fédérale de Lausanne, Campus Biotech, 1202 Geneva, Switzerland; and [e]Montreal Neurological Institute and Hospital, McGill University, Montreal, QC, Canada H3A 2B4

Orientation is a fundamental mental function that processes the relations between the behaving self to space (places), time (events), and person (people). Behavioral and neuroimaging studies have hinted at interrelations between processing of these three domains. To unravel the neurocognitive basis of orientation, we used high-resolution 7T functional MRI as 16 subjects compared their subjective distance to different places, events, or people. Analysis at the individual-subject level revealed cortical activation related to orientation in space, time, and person in a precisely localized set of structures in the precuneus, inferior parietal, and medial frontal cortex. Comparison of orientation domains revealed a consistent order of cortical activity inside the precuneus and inferior parietal lobes, with space orientation activating posterior regions, followed anteriorly by person and then time. Core regions at the precuneus and inferior parietal lobe were activated for multiple orientation domains, suggesting also common processing for orientation across domains. The medial prefrontal cortex showed a posterior activation for time and anterior for person. Finally, the default-mode network, identified in a separate resting-state scan, was active for all orientation domains and overlapped mostly with person-orientation regions. These findings suggest that mental orientation in space, time, and person is managed by a specific brain system with a highly ordered internal organization, closely related to the default-mode network.

cognitive map | disorientation | precuneus | default network | fMRI

Orientation in space, time, and person is a fundamental cognitive function and the bedrock of neurological and psychiatric mental status examination (1, 2). Orientation is defined as the "tuning between the subject and the internal representation he forms of the corresponding public reference system": that is, the external world (1). Although the representation of the external world by means of a cognitive map has been widely investigated (3–5), the way in which the self refers to this map has yet to be understood. Moreover, the behaving self refers not only to spatial landmarks but also to remembered or imagined events, or to people around, yielding a "cognitive mapping" of the time and person domains of the mental world (2, 6–9). However, it is still unknown whether mental orientation in space, time, and person relies on similar or distinct neurocognitive systems.

Several lines of research support the idea that similar neurocognitive systems underlie orientation in these three domains. Behavioral studies indicate a common psychological metric for proximity estimations ("cognitive distance") in space, time, and person (7); for example, manipulation of stimuli's distance in one orientation domain affects the perceived distance in the other two domains (10, 11). Accordingly, a recent neuroimaging study mapped cognitive distance estimations in the three domains to a single region in the inferior parietal lobe (IPL) (12). However, other neuroimaging studies that investigated processing of places, events, and people separately have found activation in brain regions besides the IPL, including the precuneus and posterior cingulate cortices, medial prefrontal cortex (mPFC), and lateral frontal and temporal lobes (6, 13–29). Notably, these regions

constitute a part of the default-mode network (DMN), a system involved in self-referential processes (24, 30–35). These findings suggest a common brain system for orientation across domains, possibly related to the DMN.

Clinical observations in patients with disorientation in space, time, and person are less clear: on the one hand, clinical syndromes may involve disorientation in several domains simultaneously, and disorientation disorders in the three domains involve lesions in similar brain regions, usually overlapping with the DMN (1, 2). On the other hand, disorientation may be limited to one specific domain – space, time, or person (2, 36–40). In addition, patients with traumatic brain injury or after electro-convulsive therapy regain their orientation gradually, from personal to spatial and temporal orientation (41, 42) whereas patients with Alzheimer's disease typically lose orientation in time first, then in place, and then in person, suggesting that partially separate systems underlie orientation in each domain.

Here, we investigated the neurocognitive system underlying orientation in space, time, and person and its relation to the DMN. To this aim, we used a mental-orientation task, with individually tailored stimuli in the space (places), time (events), and person (people) domains. To gain high anatomical specificity, we used high-resolution 7-Tesla functional MRI (fMRI). To capitalize on the spatial acuity of the high-resolution fMRI, we applied a strategy of analyzing each subject individually in native space and combined the results to compare activations for

---

## Significance

Processing of spatial, temporal, and social relations relies on mental cognitive maps, on which the behaving self is oriented relative to different places, events, and people. Using high-resolution functional MRI scanning in individual subjects, we show that mental orientation in space, time, and person produces a sequential posterior–anterior pattern of activity in each participant's brain. These activations are adjacent and partially overlapping, highlighting the relation between mental orientation in these domains. Furthermore, the activity is highly overlapping with the brain's default-mode network, a system involved in self-referential processing. These findings may shed new light on fundamental cognitive processing of space, time, and person and alter our understanding of disorientation phenomena in neuropsychiatric disorders such as Alzheimer's disease.

---

the three domains. Finally, we compared our results to the DMN as identified in each individual subject by analysis of resting-state fMRI. We hypothesized that orientation across different domains relies on a shared "core" brain system, in close relation to the DMN, yet orientation in specific domains may involve additional specialized subsystems.

## Results

### Consistent Organization of Orientation-Related Regions for Space, Time, and Person in the Precuneus, IPL, and Prefrontal Cortex.

High-resolution fMRI was recorded while subjects engaged in an orientation task, in which they viewed pairs of verbal stimuli indicating places (space domain), events (time domain), or people (person domain), and had to determine which of the two stimuli was closer to them (space, physical distance; time, time-elapsed; person, personal closeness). fMRI analysis for each domain of orientation (space, time, and person) revealed an identical pattern of brain a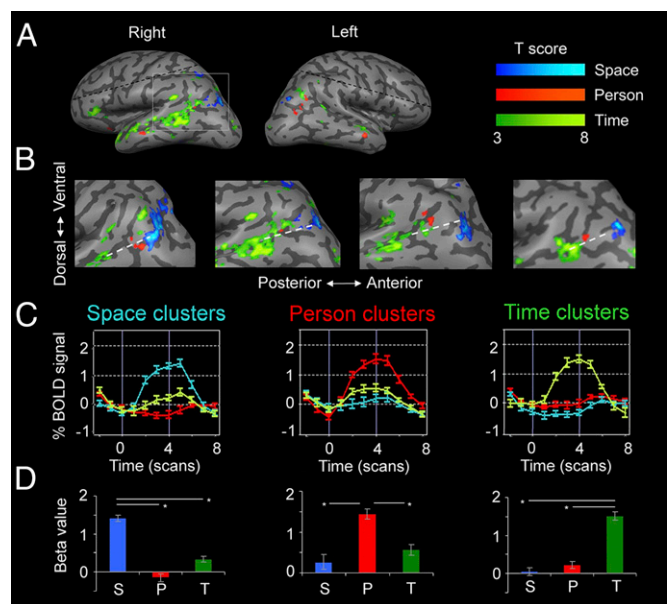ctivation for all subjects: For all three domains, activations were found in the precuneus and the adjacent posterior-cingulate cortex, regions within the IPL, and parts of the superior frontal sulcus and occipital lobe (Figs. 1 and 2 and Figs. S1 and S2). In the time and person domains, activation was additionally found at the mPFC and the superior temporal sulcus (Figs. 1 and 2 and Figs. S1 and S2).

Analysis of activations for the three domains revealed orientation-related regions, which are consistently organized in each individual subject. In all subjects, the same pattern of a
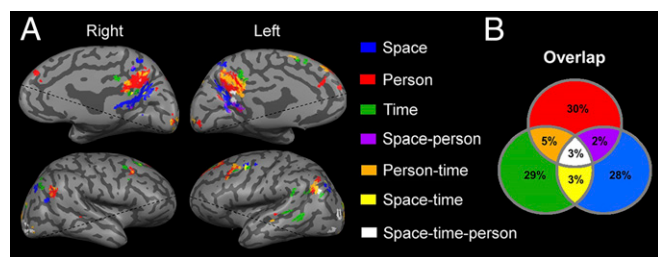


**Fig. 1.** Midsagittal cortical activity during orientation in space, time, and person. (*A*) Domain-specific activity in a representative subject, identified by contrasting activity between each orientation domain and the other two domains. The precuneus region is active in all three orientation domains, and the medial prefrontal cortex only in person and time orientation ($P < 0.05$, FDR-corrected, cluster size >20 voxels). Dashed black lines represent the limit of the scanned region in this subject. (*B*) Precuneus activity in four subjects, demonstrating a highly consistent posterior–anterior organization (white dashed line); all other subjects showed the same activity pattern (Fig. S1). (*C*) Group average (*n* = 16) of event-related activity in independent experimental runs demonstrates the specificity of each cluster to one orientation domain. Lines represent activity in response to space (blue), time (green), and person (red) conditions. Error bars represent SEM between subjects. (*D*) Group average of beta plots from volume-of-interest GLM analysis, showing highly significant domain-specific activity. Error bars represent SEM between subjects. P, person; S, space; T, time.



**Fig. 2.** Lateral cortical activity during orientation in space, time, and person. (*A*) Domain-specific activity in a representative subject, identified by contrasting activity between each orientation domain and the other two domains ($P < 0.05$, FDR-corrected, cluster size >20 voxels). The inferior parietal lobe (IPL) is active in all three orientation domains, and the temporal lobe mostly for time but also for person orientation. Notice the strong left lateralization of time activations. (*B*) IPL activity in four subjects, demonstrating a consistent posterior–anterior organization (white dashed line): All other subjects showed the same activity pattern (Fig. S1). (*C*) Group average (*n* = 16) event-related plots from independent experimental runs. (*D*) Group average of beta plots from volume-of-interest GLM analysis. See Fig. 1 legend for further details.

posterior–anterior axis of activation was found for space, person, and time, respectively. In the precuneus region, space orientation activated a posterior region around the parieto-occipital sulcus, person orientation activated the precuneus and posterior-cingulate cortex, and time orientation activated the anterior precuneus (Fig. 1 *A* and *B*) ($P < 0.05$, Wilcoxon signed-rank test). The IPL showed an identical order of posterior–anterior activation: Space orientation activated a posterior region near the intraparietal sulcus, person orientation activated posterior parts of the angular gyrus, and time orientation activated the anterior angular gyrus, extending into the temporal lobe (Fig. 2 *A* and *B*) ($P < 0.05$, Wilcoxon signed-rank test). In the mPFC, activity for person orientation was always more anterior than for time orientation ($P < 0.05$, Wilcoxon signed-rank test). Time-orientation activity was found mostly in the left hemisphere ($P < 0.01$, two-tailed paired-samples *t* test) whereas person and space activations were found bilaterally with no significant hemispheric preference ($P = 0.41$, $P = 0.26$ respectively).

To further validate the specificity of the identified activations and obtain group-level statistics, intraregional general linear model (GLM) and average event-related activity were computed for each region which had an ordered activation pattern (precuneus, IPL, mPFC) and for each orientation domain, and were compared across subjects. These results were computed from a separate experimental run than those used to identify the region of interest, ensuring that the domain-specific activation of each region was independent of its identification. These analyses showed that the domain-specific regions of interest responded consistently and specifically to their preferred orientation domain and not to other domains, across all subjects and regions (all *P* values < 0.001, Tukey–Kramer post hoc test) (Figs. 1 *C* and *D* and 2 *C* and *D*). Finally, we performed a random-effects

NEUROSCIENCE

PSYCHOLOGICAL AND COGNITIVE SCIENCES

**Fig. 3.** Overlap between activations in the space, time, and person domains. (A) Overall orientation-related activity in a representative subject, identified by contrasting activity between each orientation domain and the lexical control task, showing overlap between regions ($P < 0.05$, FDR-corrected, cluster size >20 voxels). (B) Group average of the percent of overlap between active voxels in each orientation domain, demonstrating a partial overlap between domains (for group-level results, see Figs. S3B and S4B).

GLM group analysis and a probabilistic-maps group analysis (Figs. S3A and S4A): results were found to be similar to those obtained from single subjects.

Subjects' response time, level of emotional valence, stimuli length, past-versus-future events, and distance of stimuli from the subject's self-location in space, time, or person may also affect our results. Addition of regressors to the design matrix for each potential confound ruled out such effects on orientation-related activations (*SI Methods, SI Results*, and Table S1).

**Interrelations Between Orientation-Related Regions in Space, Time, and Person.** The finding of domain-selective regions for orientation revealed a partial anatomical segregation between them. To determine the interrelations between domains, we contrasted each domain's activity with a lexical control task and checked for overlapping activations. At the individual subject level, most voxels (87%) were found to be domain-specific, and 13% of the voxels were activated in response to two or three domains (Fig. 3; for detailed percentages, see Fig. 3B). At the group level, analyses demonstrated overlap of 28% between domains in the precuneus region and IPL (Figs. S3B and S4B). Analysis of the average gap between orientation-related activations revealed no gaps when considering the full extent of orientation-related regions and a gap of 1–7 mm between domain-specific regions in the precuneus and lateral parietal lobe (Table S2). The results of these overlap and adjacency analyses suggest the existence of core processing for the different orientation domains.
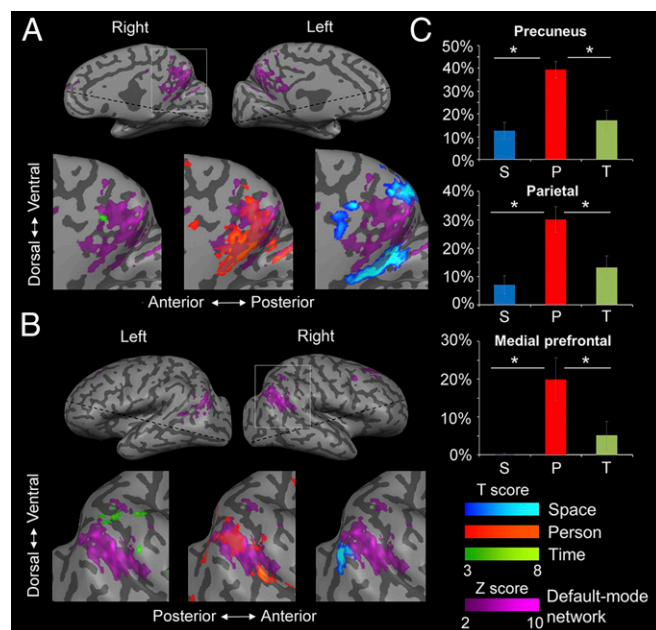
**The DMN Partially Overlaps with Orientation-Related Regions.** The DMN has been suggested to process "aspects of the [multifaceted] self" (31) and was hypothesized to relate to self-projection in space, time, and person (33), similarly to the orientation system. In view of this resemblance, as well as the similarity of the regions we have identified here and the DMN, we examined the relation between the two systems. The DMN was identified in a separate resting-state run, using independent-components analysis (ICA) for each individual subject, and was compared with subjects' orientation-related regions (Fig. 4). This comparison demonstrated a significant overlap in the precuneus region because 50% of DMN voxels were active during mental orientation (identified using the contrast between each orientation domain and the other two domains). Overlap was also evident in the IPL and mPFC (14% and 17% of voxels, respectively) (Figs. S5–S8). We next tested the relation between the DMN and regions related to each domain (space, time, and person): Most of the DMN voxels active during orientation were within person-orientation regions (32%), significantly more than in space (12%) and time (10%) regions, across the whole brain ($P < 0.01$, Tukey–Kramer post hoc test) (Fig. 4). Finally, we tested the activity in

each DMN node (precuneus, IPL, and mPFC, as identified in the resting-state scan) in response to the orientation task in each domain; the IPL and precuneus nodes were active for all domains with similar average blood oxygenation level-dependent (BOLD) signal strength, and the mPFC for the person domain (Fig. S9).

## Discussion

Functional examination of brain activity during orientation in space, time, and person revealed several findings. Specific regions were found to be active for each orientation domain (space, time, or person) in the precuneus and posterior cingulate cortex, IPL, mPFC, and lateral frontal and lateral temporal cortices. These domain-specific regions are adjacent and partially overlapping and are organized along a posterior–anterior axis. Finally, all orientation-related regions have a prominent overlap with the DMN, and DMN nodes responded similarly to the different orientation domains.

The question of whether orientation in space, time, and person relies on a common brain system is under debate (1, 2). The regions we have identified—precuneus and posterior cingulate cortex, IPL, mPFC and lateral temporal and frontal lobes—have been implicated in self-related aspects of space (navigation) (13–17), time (autobiographical memory) (18–21), and person (representation of self and others) (22–25, 27–29). In addition, these regions are involved in specifying relations between landmarks in each domain: cognitive mapping of the spatial environment, recency judgments of life-events, and social proximity and hierarchy judgments (13, 16, 43–46). However, most previous studies investigated a single domain (space, time, or person). Here, we directly compared activity between orientation domains in individual subjects using high-resolution imaging. Comparison of each orientation domain with the other two domains enabled segregation of domain-specific regions



**Fig. 4.** Overlap of orientation activity with the default mode network (DMN). The DMN was identified using resting-state fMRI in each individual subject. The DMN is presented for a representative subject, overlaid with activity during the orientation task in space, time, and person (identified by contrasting activity between each orientation domain and the other two domains). (A) Midsagittal view, focus on the precuneus. (B) Lateral view, focus on the IPL. (C) Average percent, across subjects, of DMN voxels from all voxels active specifically for a single orientation domain. DMN voxels were found most prominently in the person domain (two-tailed $t$ test, all $P < 0.01$) although some were found also in the time and space domains. P, person; S, space; T, time.

of orientation. These regions were adjacent to each other (especially in the precuneus region), as demonstrated by gap analysis between activation-specific regions. Moreover, comparison of each domain to a lexical control task revealed a significant overlap between the different orientation domains. Finally, activations for the three domains showed a similar pattern inside the precuneus and IPL nodes of the DMN. Taken together, these findings suggest that orientation domains have an intrinsic organization in the precuneus region, IPL, and mPFC and support a model of a general orientation system with distinct domain-specific divisions and a common functional core (although the different activations may also overlap additional different global brain systems). These findings can be explained by the general function of orientation, which processes the relation between the self and externally cued stimuli. Orientation may therefore require a coupling of activation between core regions involved in self-related processing, with cortical regions required for domain-specific computations. The organization pattern of adjacent and partially overlapping regions for orientation in different domains may further reflect the principle of anatomical duplication, or "recycling," of an existing cortical system in the course of evolution, to be used in new roles or domains (47, 48). In such a conceptual framework, it may be speculated that a primitive biological mechanism for spatial representation may have been used to represent other domains such as time and person, and the relevant brain regions may have gradually diverged and become partially segregated (8, 9, 47, 49).

The anatomical adjacency and overlap between space, time, and person regions adds neuroanatomical evidence for the interrelations between these domains on the cognitive level. Large-scale spatial representations are thought to rely on a "cognitive map" (3), which combines continuous representations of space with its hierarchical separation into segments (e.g., neighborhoods, cities, states, etc.) (50–52), and is partially dependent on the observer's reference point (53). Time representation relies on a representation of a continuous "time line" (54), with segmentation into time periods (55), and is also affected by the reference point (6, 56). Person (social) relations are categorized into groups (57), their perception is affected by personal point-of-view (58), and possible parallels may exist for a continuous-line representation of "social space" or a "social cognitive map" (8). In addition, behavioral tests demonstrated interactions between space, time, and person in cognitive-distance estimations, priming, and interference (9–11). These relations led to the formulation of the Construal Level Theory, which posits that places, events, and people are represented by a single self-referenced cognitive system and that distance estimations in this system are directly related to the level of abstractness of the stimuli (7). Our findings support the idea that orientation in space, time, and person is represented by related and interacting cognitive systems; however, we demonstrate that these systems are not completely identical but are separated into subsystems specific for each domain.

Our study demonstrated that activity in the DMN overlaps with the orientation system. The DMN was first described as a system that is deactivated during cognitive tasks (30). However, further investigations uncovered a set of self-referential tasks that activate the DMN—including self-projection, memory, social representation, navigation, and internally directed thoughts (21, 24, 28, 31, 34, 35). Our orientation task also activates the DMN, compatible with the self-referential nature of both systems. Interestingly, our data shows that the DMN spatially overlaps mainly person-orientation regions, unlike previous hypotheses (31). This specialization of the DMN in personal content and relations may reflect the central role of personal and social content in mental life (59). The DMN may therefore serve orientation processes by providing self-referenced content or perspectives in the different domains, with an emphasis on personal content (28). Analysis of averaged activation revealed the precuneus and IPL DMN nodes to be active for all orientation

domains; the mPFC node was active for the person domain, in agreement with previous studies (23, 25, 31). The findings of similar DMN activity across domains strengthen the evidence for interrelations between the different orientation domains. The domain-general activity of the DMN, together with the findings of overlap between activations, suggests that mental orientation may be accomplished through coactivation of core DMN regions, which enables self-related processing, together with cortical regions involved in domain-specific computations that relate to representation of the "extrinsic" world to which the self is related.

Interestingly, recent large-scale studies have also identified three subsystems in the DMN (60–62), with similar topography to the domain-specific regions as found here. Although we interpret our results with regard to mental orientation in the different domains (space, time, and person), data recorded in previous studies was interpreted at another level of description regarding its cognitive functions: constructive mental simulation for the system corresponding to space-orientation regions, construction of personal meaning for person-orientation regions, and semantic/conceptual processing for time-orientation regions. These differences may be related to differential recruitment of these core functional processes for each orientation domain. Such an interpretation may be especially relevant to regions specifically active for one orientation domain with a well-defined functional role, such as the temporal lobe for semantic memory (63, 64), which may be involved in time orientation. Future work is needed to further explain how well-known cognitive processes are involved in orientation to different domains. Furthermore, application of both domain-general and domain-specific contrasts enabled us to identify areas of convergence between the three subsystems, a major principle in the organization of the DMN (61), which merits further investigation.

Our investigation revealed several additional findings. First, the time-orientation system is strongly left-lateralized, with prominent activity along the entire length of the superior temporal sulcus, corroborating previous studies (6, 19, 43, 56, 65, 66). Second, the spatial-orientation system was located posteriorly, with no involvement of the frontal lobe, and converged medially on the parieto-occipital sulcus (sometimes referred to as the retrosplenial cortex), consistent with previous findings (16, 17, 36, 67). This finding is also in line with the suggested separation of the DMN into dorsal and ventral routes, of which the ventral is focused on spatial navigation and scene construction, and the dorsal on social cognitive processes (61, 68). Finally, no orientation domain activated the hippocampus, despite its undisputed role in spatial and temporal representation, navigation, and cognitive mapping (4, 5, 69). This finding may be related to the self-referential (egocentric) nature of our task whereas the hippocampus is considered to serve allocentric representations (5, 14); alternatively, it may relate to the use of existing large-scale mental maps whereas the hippocampus is more active during navigation and encoding of the immediate environment (5, 15).

Disturbances of orientation are evident in many neuropsychiatric disorders (1, 2). In a previous investigation, we characterized 22 types of disorientation disorders and classified them as affecting a single orientation domain or several domains simultaneously (2). Our finding of separate but anatomically adjacent and overlapping regions for orientation in space, time, and person may explain this pattern of lesion–symptom correlation, in which circumscribed brain lesions may affect only a specific orientation domain, but more extensive lesions may lead to disorientation in several domains. Lesion studies further support the regions we identified: For example, localized damage to the parieto-occipital region can lead to "heading orientation"—a specific impairment in the spatial cognitive map, without accompanying disorientation in time and person (36, 37); lesions in left temporo-parietal regions and temporal-lobe epilepsy can induce specific disorientation in time, consistent with the above-described

findings (2, 65, 70). An important disorder of orientation is Alzheimer's disease, in which disorientation in space, time, and person is a hallmark. Disorientation in Alzheimer's disease may be understood in view of the interrelation between the DMN and the orientation system because the DMN has a major involvement in the neuropathology of Alzheimer's disease (71, 72).

Despite our systematic findings, this study is not free of limitations. Mental orientation relies on (*i*) representation of the large-scale environment (places, events, and people), and (*ii*) self-reference to these representations; our task involves these two components of orientation and cannot dissociate between regions responsible for their processing. In addition, the processing of space, time, and person may invoke additional mental processes specific to each of these domains that are not related to orientation, as defined here. We attempted to minimize these effects by choosing a task that focused on orientation processing in each domain (self-referenced cognitive distance) and also controlled for various variables that may differ between domains. However, we cannot completely exclude such domain-specific effects in our data. The use of individual-subject ICA may introduce noise into the DMN components, which are furthermore threshold-dependent; therefore, the exact percentage of overlap between orientation domains and DMN is hard to ascertain. However, our main results of significant preferential overlap with the person domain and DMN activity for all orientation domains are independent of, and cannot be explained by, this accuracy limit. Finally, despite the steps taken to prevent recall of the stimuli from the prescan session and subjects' reports, we cannot completely rule out involvement of recall processes in our results.

In conclusion, this study identified brain regions underlying the cognitive function of mental orientation, which relates the behaving self to its surrounding in the space, time, and person domains. These regions follow a strict internal organization, with distinct domain-specific subdivisions and a common functional core, and are closely related to the DMN. Future research may deepen our understanding of mental orientation and its modes of operation in neuropsychiatric disorders.

## Methods

**Subjects.** Sixteen healthy right-handed subjects (eleven males, mean age 23.9 ± 3.9 y) participated in the study. All subjects provided written informed consent, and the study was approved by the ethical committee of the Canton of Vaud, Switzerland.

**Experimental Paradigm.** The same experimental task was used in all three orientation domains. Stimuli consisted of names of cities (space), events (time), or people (person) (stimuli are fully described in *SI Methods*). Subjects were presented with two stimuli from the same domain (space, time, or person) and were asked to determine which of the two stimuli is closer to them: spatially closer to their current location (for space stimuli), temporally closer to the current time (for time stimuli), or personally closer to themselves (for person stimuli). Therefore, the task and instructions were similar for each orientation domain (space, time, person). To control for distance and difficulty effects (response-time facilitation for stimuli farther apart from each other) (51), subjects' estimates of stimulus's distances were used to select pairs of stimuli with adjacent distances.

Stimuli pairs were presented in a randomized block design, each block containing four consecutive stimuli pairs of a specific orientation domain and distance. Each pair was presented for 2.5 s, and each block (10 s) was followed by 10 s of fixation. Subjects were instructed to respond accurately but as fast as possible. A 5-min training task containing different stimuli was delivered before the experiment. The experiment comprised five experimental runs, each containing 18 blocks in a randomized order. In addition, subjects performed a lexical control task in a separate run, in which they viewed similar stimuli pairs but were instructed to indicate whether or not any of the words contained the letter "T." Stimuli were presented using the ExpyVR software (lnco.epfl.ch/expyvr). After the experiment, subjects rated each task's difficulty, the strategy used, the emotional valence of each stimulus (from 1 to 10), and whether each event was a future or past event. In the inquiry after the experiment, all participants reported not trying to recall these stimuli ratings during the experiment.

**Functional MRI Analysis.** MRI acquisition and preprocessing are described in *SI Methods*.

*Identification of domain-specific and domain-general activity.* A GLM analysis (73) was applied to each subject separately in native space (for full details see *SI Methods*). To identify activations specific to each orientation domain, we used a balanced contrast between each specific orientation domain (space, time, person) and the average of the other two domains. This contrast identified regions responding specifically to only one orientation domain. To identify the full extent of activation for each domain, we contrasted each orientation domain with the lexical control task. This second contrast enabled detection of overlap of activations between several domains. Finally, to exclude activations which did not rise above baseline, a conjunction analysis was performed for each of these contrasts with an additional contrast between the specific orientation domain and rest (baseline). Activation regions-of-interest were classified as belonging to separate brain regions (precuneus, parietal, etc.) as detailed in *SI Methods*.

*Group-level analysis.* To validate the specificity of the activation clusters at the group level, activation clusters were isolated in each subject using the above-mentioned contrasts [$P < 0.05$, false discovery rate (FDR)-corrected], with a minimal threshold of 300 voxels. Clusters were grouped according to their anatomical region (precuneus region, inferior parietal, medial or lateral frontal, lateral temporal). A GLM analysis was run for each subject inside each anatomical region, after correction for serial correlations, normalization to the percent of signal change, and addition of motion parameters to the GLM. To avoid circular-analysis bias, the activation clusters were identified using only four of the five experimental runs, and the remaining (independent) run was used for the GLM computation. ANOVAs with Tukey–Kramer post hoc tests were used to compare the beta values for each domain with the beta values for the other two domains, across all subjects. In addition, event-related responses were averaged for each condition, in each activation cluster (again using four runs for cluster identification and the fifth for response measurement). The event-related responses were averaged across subjects to obtain a characteristic response. Event-related averages were additionally computed for each DMN node, using data from all experimental runs. Finally, random-effects GLM and probabilistic-maps analyses were performed on all subjects after spatial normalization and smoothing, to obtain further group-level results (*SI Methods*).

*Overlap of domain-specific activity and the DMN.* Independent components analysis (ICA) with 30 eigenvalues was performed on resting-state scans (74), using a gray-matter mask to reduce noncortical noise. The DMN was identified by searching for a component that included the medial prefrontal, posterior cingulate, and inferior parietal cortices. A component clearly corresponding to the DMN was identified in 13 of the 16 subjects (Figs. S5–S7); in the remaining three, no DMN component could be identified, and they were therefore excluded from this analysis. Overall overlap between the DMN and orientation-related regions was computed by counting DMN voxels that were active in a specific domain (identified using a contrast between each orientation domain and the other two domains) and dividing by the total number of DMN voxels. The opposite overlap percentage was computed by counting DMN voxels that showed domain-specific activity (contrast between each orientation domain and the other two domains) and dividing by the sum of all domain-specific active voxels.

1. Berrios GE (1982) Disorientation states and psychiatry. *Compr Psychiatry* 23(5): 479–491.

2. Peer M, Lyon R, Arzy S (2014) Orientation and disorientation: Lessons from patients with epilepsy. *Epilepsy Behav* 41:149–157.

3. Tolman EC (1948) Cognitive maps in rats and men. *Psychol Rev* 55(4):189–208.

4. O'Keefe J, Nadel L (1978) *The Hippocampus as a Cognitive Map* (Clarendon Press, Oxford).

5. Burgess N, Maguire EA, O'Keefe J (2002) The human hippocampus and spatial and episodic memory. *Neuron* 35(4):625–641.

6. Arzy S, Collette S, Ionta S, Fornari E, Blanke O (2009) Subjective mental time: The functional architecture of projecting the self to past and future. *Eur J Neurosci* 30(10):2009–2017.

7. Liberman N, Trope Y (2008) The psychology of transcending the here and now. *Science* 322(5905):1201–1205.

8. Parkinson C, Wheatley T (2013) Old cortex, new contexts: Re-purposing spatial perception for social cognition. *Front Hum Neurosci* 7:645.

9. Boroditsky L (2000) Metaphoric structuring: Understanding time through spatial metaphors. *Cognition* 75(1):1–28.

10. Bar-Anan Y, Liberman N, Trope Y, Algom D (2007) Automatic processing of psychological distance: Evidence from a Stroop task. *J Exp Psychol Gen* 136(4):610–622.

11. Maglio SJ, Trope Y, Liberman N (2013) Distance from a distance: Psychological distance reduces sensitivity to any further psychological distance. *J Exp Psychol Gen* 142(3):644–657.

12. Parkinson C, Liu S, Wheatley T (2014) A common cortical metric for spatial, temporal, and social distance. *J Neurosci* 34(5):1979–1987.

13. Maguire EA, et al. (1998) Knowing where and getting there: A human navigation network. *Science* 280(5365):921–924.

14. Burgess N, Maguire EA, Spiers HJ, O'Keefe J (2001) A temporoparietal and prefrontal network for retrieving the spatial context of lifelike events. *Neuroimage* 14(2):439–453.

15. Rosenbaum RS, Ziegler M, Winocur G, Grady CL, Moscovitch M (2004) "I have often walked down this street before": fMRI studies on the hippocampus and other structures during mental navigation of an old environment. *Hippocampus* 14(7):826–835.

16. Epstein RA, Parker WE, Feiler AM (2007) Where am I now? Distinct roles for parahippocampal and retrosplenial cortices in place recognition. *J Neurosci* 27(23):6141–6149.

17. Vann SD, Aggleton JP, Maguire EA (2009) What does the retrosplenial cortex do? *Nat Rev Neurosci* 10(11):792–802.

18. Cabeza R, et al. (1997) Brain regions differentially involved in remembering what and when: A PET study. *Neuron* 19(4):863–870.

19. Svoboda E, McKinnon MC, Levine B (2006) The functional neuroanatomy of autobiographical memory: A meta-analysis. *Neuropsychologia* 44(12):2189–2208.

20. Schacter DL, Addis DR, Buckner RL (2007) Remembering the past to imagine the future: The prospective brain. *Nat Rev Neurosci* 8(9):657–661.

21. Spreng RN, Mar RA, Kim ASN (2009) The common neural basis of autobiographical memory, prospection, navigation, theory of mind, and the default mode: A quantitative meta-analysis. *J Cogn Neurosci* 21(3):489–510.

22. Saxe R, Kanwisher N (2003) People thinking about thinking people: The role of the temporo-parietal junction in "theory of mind". *Neuroimage* 19(4):1835–1842.

23. Mitchell JP, Banaji MR, Macrae CN (2005) The link between social cognition and self-referential thought in the medial prefrontal cortex. *J Cogn Neurosci* 17(8):1306–1315.

24. Goldberg II, Harel M, Malach R (2006) When the brain loses its self: Prefrontal inactivation during sensorimotor processing. *Neuron* 50(2):329–339.

25. Heatherton TF, et al. (2006) Medial prefrontal activity differentiates self from close others. *Soc Cogn Affect Neurosci* 1(1):18–25.

26. Arzy S, Thut G, Mohr C, Michel CM, Blanke O (2006) Neural basis of embodiment: Distinct contributions of temporoparietal junction and extrastriate body area. *J Neurosci* 26(31):8074–8081.

27. Carter RM, Bowling DL, Reeck C, Huettel SA (2012) A distinct role of the temporal-parietal junction in predicting socially guided decisions. *Science* 337(6090):109–111.

28. Salomon R, Levy DR, Malach R (2014) Deconstructing the default: Cortical subdivision of the default mode/intrinsic system during self-related processing. *Hum Brain Mapp* 35(4):1491–1502.

29. Hassabis D, et al. (2014) Imagine all the people: How the brain creates and uses personality models to predict behavior. *Cereb Cortex* 24(8):1979–1987.

30. Raichle ME, et al. (2001) A default mode of brain function. *Proc Natl Acad Sci USA* 98(2):676–682.

31. Gusnard DA, Akbudak E, Shulman GL, Raichle ME (2001) Medial prefrontal cortex and self-referential mental activity: Relation to a default mode of brain function. *Proc Natl Acad Sci USA* 98(7):4259–4264.

32. Salomon R, Malach R, Lamy D (2009) Involvement of the intrinsic/default system in movement-related self recognition. *PLoS One* 4(10):e7527.

33. Buckner RL, Carroll DC (2007) Self-projection and the brain. *Trends Cogn Sci* 11(2):49–57.

34. Christoff K, Gordon AM, Smallwood J, Smith R, Schooler JW (2009) Experience sampling during fMRI reveals default network and executive system contributions to mind wandering. *Proc Natl Acad Sci USA* 106(21):8719–8724.

35. Smallwood J, Brown K, Baird B, Schooler JW (2012) Cooperation between the default mode network and the frontal-parietal network in the production of an internal train of thought. *Brain Res* 1428:60–70.

36. Takahashi N, Kawamura M, Shiota J, Kasahata N, Hirayama K (1997) Pure topographic disorientation due to right retrosplenial lesion. *Neurology* 49(2):464–469.

37. Aguirre GK, D'Esposito M (1999) Topographical disorientation: A synthesis and taxonomy. *Brain* 122(Pt 9):1613–1628.

38. Arzy S, Bick A, Blanke O (2009) Mental time in amnesia: Evidence from bilateral medial temporal damage before and after recovery. *Cogn Neuropsychol* 26(6):503–510.

39. O'Keeffe E, Mukhtar O, O'Keeffe ST (2011) Orientation to time as a guide to the presence and severity of cognitive impairment in older hospital patients. *J Neurol Neurosurg Psychiatry* 82(5):500–504.

40. Förstl H, Almeida OP, Owen AM, Burns A, Howard R (1991) Psychiatric, neurological and medical aspects of misidentification syndromes: A review of 260 cases. *Psychol Med* 21(4):905–910.

41. Tate RL, Pfaff A, Jurjevic L (2000) Resolution of disorientation and amnesia during post-traumatic amnesia. *J Neurol Neurosurg Psychiatry* 68(2):178–185.

42. Daniel WF, Crovitz HF, Weiner RD (1987) Neuropsychological aspects of disorientation. *Cortex* 23(2):169–187.

43. St Jacques P, Rubin DC, LaBar KS, Cabeza R (2008) The short and long of it: Neural correlates of temporal-order memory for autobiographical events. *J Cogn Neurosci* 20(7):1327–1341.

44. Kimura HM, et al. (2010) Differential temporo-parietal cortical networks that support relational and item-based recency judgments. *Neuroimage* 49(4):3474–3480.

45. Farrow TFD, et al. (2011) Higher or lower? The functional anatomy of perceived allocentric social hierarchies. *Neuroimage* 57(4):1552–1560.

46. Mason M, Magee JC, Fiske ST (2014) Neural substrates of social status inference: Roles of medial prefrontal cortex and superior temporal sulcus. *J Cogn Neurosci* 26(5):1131–1140.

47. Dehaene S, Cohen L (2007) Cultural recycling of cortical maps. *Neuron* 56(2):384–398.

48. Anderson ML (2010) Neural reuse: A fundamental organizational principle of the brain. *Behav Brain Sci* 33(4):245–266, discussion 266–313.

49. Casasanto D, Boroditsky L (2008) Time in the mind: Using space to think about time. *Cognition* 106(2):579–593.

50. Kosslyn SM, Murphy GL, Bemesderfer ME, Feinstein KJ (1977) Category and continuum in mental comparisons. *J Exp Psychol Gen* 106(4):341–375.

51. Maki RH (1981) Categorization and distance effects with spatial linear orders. *J Exp Psychol Hum Learn* 7(1):15–32.

52. McNamara TP (1986) Mental representations of spatial relations. *Cognit Psychol* 18(1):87–121.

53. Holyoak KJ, Mah WA (1982) Cognitive reference points in judgments of symbolic magnitude. *Cognit Psychol* 14(3):328–352.

54. Arzy S, Adi-Japha E, Blanke O (2009) The mental time line: An analogue of the mental number line in the mapping of life events. *Conscious Cogn* 18(3):781–785.

55. Grondin S (2001) From physical time to the first and second moments of psychological time. *Psychol Bull* 127(1):22–44.

56. Arzy S, Molnar-Szakacs I, Blanke O (2008) Self in time: Imagined self-location influences neural activity related to mental time travel. *J Neurosci* 28(25):6502–6507.

57. Macrae CN, Bodenhausen GV (2000) Social cognition: Thinking categorically about others. *Annu Rev Psychol* 51(1):93–120.

58. Maister L, Slater M, Sanchez-Vives MV, Tsakiris M (2015) Changing bodies changes minds: Owning another body affects social cognition. *Trends Cogn Sci* 19(1):6–12.

59. Dunbar RI (1998) The social brain hypothesis. *Brain* 9(10):178–190.

60. Andrews-Hanna JR, Smallwood J, Spreng RN (2014) The default network and self-generated thought: Component processes, dynamic control, and clinical relevance. *Ann N Y Acad Sci* 1316(1):29–52.

61. Andrews-Hanna JR, Reidler JS, Sepulcre J, Poulin R, Buckner RL (2010) Functional-anatomic fractionation of the brain's default network. *Neuron* 65(4):550–562.

62. Yeo BTT, et al. (2011) The organization of the human cerebral cortex estimated by intrinsic functional connectivity. *J Neurophysiol* 106(3):1125–1165.

63. Binder JR, Desai RH (2011) The neurobiology of semantic memory. *Trends Cogn Sci* 15(11):527–536.

64. Patterson K, Nestor PJ, Rogers TT (2007) Where do you know what you know? The representation of semantic knowledge in the human brain. *Nat Rev Neurosci* 8(12):976–987.

65. Spiers HJ, et al. (2001) Unilateral temporal lobectomy patients show lateralized topographical and episodic memory deficits in a virtual town. *Brain* 124(Pt 12):2476–2489.

66. Konishi S, Asari T, Jimura K, Chikazoe J, Miyashita Y (2006) Activation shift from medial to lateral temporal cortex associated with recency judgements following impoverished encoding. *Cereb Cortex* 16(4):469–474.

67. Ino T, et al. (2002) Mental navigation in humans is processed in the anterior bank of the parieto-occipital sulcus. *Neurosci Lett* 322(3):182–186.

68. Kahn I, Andrews-Hanna JR, Vincent JL, Snyder AZ, Buckner RL (2008) Distinct cortical anatomy linked to subregions of the medial temporal lobe revealed by intrinsic functional connectivity. *J Neurophysiol* 100(1):129–139.

69. Buzsáki G, Moser EI (2013) Memory, navigation and theta rhythm in the hippocampal-entorhinal system. *Nat Neurosci* 16(2):130–138.

70. Bear DM, Fedio P (1977) Quantitative analysis of interictal behavior in temporal lobe epilepsy. *Arch Neurol* 34(8):454–467.

71. Greicius MD, Srivastava G, Reiss AL, Menon V (2004) Default-mode network activity distinguishes Alzheimer's disease from healthy aging: Evidence from functional MRI. *Proc Natl Acad Sci USA* 101(13):4637–4642.

72. Buckner RL, et al. (2005) Molecular, structural, and functional characterization of Alzheimer's disease: Evidence for a relationship between default activity, amyloid, and memory. *J Neurosci* 25(34):7709–7717.

73. Friston KJ, et al. (1994) Statistical parametric maps in functional imaging: A general linear approach. *Hum Brain Mapp* 2(3):189–210.

74. McKeown MJ, et al. (1998) Analysis of fMRI data by blind separation into independent spatial components. *Hum Brain Mapp* 6(3):160–188.

75. Salomon R, Darulova J, Narsude M, van der Zwaag W (2014) Comparison of an 8-channel and a 32-channel coil for high-resolution FMRI at 7 T. *Brain Topogr* 27(2):209–212.

76. Marques JP, et al. (2010) MP2RAGE, a self bias-field corrected sequence for improved segmentation and T1-mapping at high field. *Neuroimage* 49(2):1271–1281.

77. Shah NJ, et al. (2001) The neural correlates of person familiarity: A functional magnetic resonance imaging study with clinical implications. *Brain* 124(Pt 4):804–815.

# Supporting Information

## Peer et al. 10.1073/pnas.1504242112

### SI Methods

**Experimental Stimuli.** Space stimuli consisted of names of cities in Europe, distanced 50–1,500 km from the experimental location (Lausanne, Switzerland). Time stimuli consisted of two-word descriptions of common events from personal life (e.g., final examinations) or nonpersonal world events (e.g., Obama's election), as well as potential future events of both types (e.g., first child, Mars landing). Person stimuli consisted of names of people, personally familiar to the subject (family members, friends) or famous people (e.g., Barack Obama, Julia Roberts). Several days before the experiment, participants received a questionnaire and were asked to estimate their spatial distance from each location, temporal distance from each event, and personal distance from each person, on a scale of one to seven, giving rise to seven distance categories. Stimuli were selected from the original questionnaire to obtain five stimuli from each of the seven categories (35 stimuli in total for each domain). To avoid memorization of stimuli, 210 stimuli were rated and only 105 were selected for use in the experiment. To ascertain the consistency of subjects' distance rating, nine subjects were asked to reevaluate the distances 2–3 wk after the experiment; no significant differences were found between the two ratings ($P > 0.44$), and the average absolute difference in rating was smaller than 1.

**MRI Acquisition.** Subjects were scanned in a 7T Magnetom Siemens MRI (Siemens Medical Solutions) at the Center for Biomedical Imaging institute at École Polytechnique Fédérale de Lausanne using a 32-channel coil (Nova Medical) to obtain high-resolution functional scans (75). Blood oxygenation level-dependent (BOLD) contrast was obtained with a gradient-echo echo-planar imaging sequence [repetition time (TR), 2,500; echo time (TE), 25 ms; flip angle, 75°; field of view, 208 mm; matrix size, 124 × 124; functional voxel size, 1.7 × 1.7 × 1.7 mm; generalized autocalibrating partially parallel acquisition, 2]. The scanned volume included 45 axial slices of 1.7 mm thickness with no gap. The high resolution of the scan did not allow for whole-brain coverage, and therefore the scan was limited in the first 10 subjects to the frontal, parietal, and occipital lobes, excluding the temporal pole, anterior medial and lateral temporal lobe, and the orbitofrontal cortex. In the other 6 subjects, the scan included the temporal, parietal, and occipital lobes but excluded the dorsal prefrontal cortex. BOLD scans consisted of six runs (five orientation runs and a lexical control run), each consisting of 160 TRs. In addition, a resting state scan of 120 TRs with identical parameters was performed. T1-weighted high-resolution (1 mm × 1 mm × 1 mm, 176 slices) anatomical images were also acquired for each subject using the MP2RAGE protocol (76) [TR, 5,500 ms; TE, 2.84 ms; flip angle, 75°; field of view, 256 mm; inversion time 1 (TI1), 750 ms; TI2, 2,350 ms].

**MRI Preprocessing.** fMRI data were analyzed using the BrainVoyager software package (R. Goebel, Brain Innovation, Masstricht, The Netherlands), Neuroelf (www.neuroelf.net), and in-house, Matlab-based software. Preprocessing of functional scans included 3D motion correction by realignment to the first image in the first run, high-pass filtering (up to two cycles in the task scans and 0.005 Hz in the resting-state scan), exclusion of voxels below intensity values of 100, and coregistration to the anatomical T1 images. Runs with maximal motion above a single voxel size (1.7 mm) in any direction were removed from further analyses. Anatomical brain images were corrected for signal inhomogeneity, skull-stripped, and transformed to anterior commissure–posterior commissure orientation. No spatial smoothing or normalization of the

voxels was performed, to preserve the high resolution and specificity of individual-subject activity.

**Functional MRI analysis.** To assess the selective activations elicited by different experimental tasks, we applied a general linear model (GLM) analysis (73). Predictors were constructed for all conditions, convoluted with a canonical hemodynamic response function, and the model was independently fitted to the time course of each voxel. Motion parameters were added to the GLM to remove motion-related noise. Analyses were performed for each subject separately in native space, in a fixed-effect manner by joining the different experimental runs. Data were further corrected for serial correlations and transformed to units of percent signal change.

**Anatomical classification of activation clusters.** Activations were classified as belonging to one of four regions: (*i*) the precuneus region—bordered by the marginal, callosal and parieto-occipital sulci, including the cortex inside these sulci; (*ii*) the prefrontal lobe—anterior to the precentral sulcus laterally and paracentral sulcus medially; (*iii*) the inferior parietal lobe—posterior to the postcentral sulcus and lateral to the intraparietal sulcus; and (*iv*) the lateral temporal lobe—anterior to a line drawn between the posterior end of the lateral sulcus and the preoccipital notch. This grouping in each orientation domain separately was used for the analyses of event-related averaging, activation overlap and adjacency analyses, and beta-value extraction from region-of-interest GLM.

**Random-effects and probabilistic-maps group analyses.** Subjects' functional data were normalized into Talairach space and smoothed using an 8-mm Gaussian kernel. Random-effects analysis was performed on all 16 subjects using the BrainVoyager software. To observe activations in the temporal and frontal lobes, which were scanned in a partial sample of the subjects, probabilistic-maps analysis was performed on these subjects (10 subjects for frontal lobe, 6 for temporal lobe); individual-subjects maps used for this analysis were FDR-corrected and cluster size-thresholded at 20 voxels.

**Validation of posterior–anterior order-of-activation clusters.** Centers of mass were computed for each activation cluster (contrast between each domain and the other two domains) in the precuneus/parietal lobe. Precuneus clusters were rotated by −45° to obtain a rostral–caudal orientation. In each subject where all three clusters (space, time, and person) were identifiable, each cluster's location on the *y* axis was compared with the other two clusters across subjects using Wilcoxon's signed-rank tests (separately for the precuneus region and parietal lobe).

**Identification of hemispheric preference.** For each contrast, all of the active voxels were segregated into right and left hemisphere activations using BrainVoyager automatic hemisphere segregation. Voxels were counted in each hemisphere and compared using two-tailed paired-sample *t* test to identify laterality preferences.

**Interdomain overlap.** To identify overlap between regions, activation clusters were isolated from the contrast between each domain and the control task, as described above. Overlap was computed by the percent of voxels significantly active in two or three of the contrasts, compared with the total number of active voxels. Percentages of overlapping voxels were averaged across subjects.

**Interdomain adjacency and gaps.** Gaps were computed as the minimal Euclidean distance between the borders of each pair of clusters, in each hemisphere separately. In the case of overlapping activity, overlap extent (maximal Euclidean distance between activation borders inside the overlapping region) was represented by a negative value. Activation clusters were taken from results of the contrast between each domain and the lexical control (Fig. 3 and Fig. S3) and the contrast between each domain and the other two domains
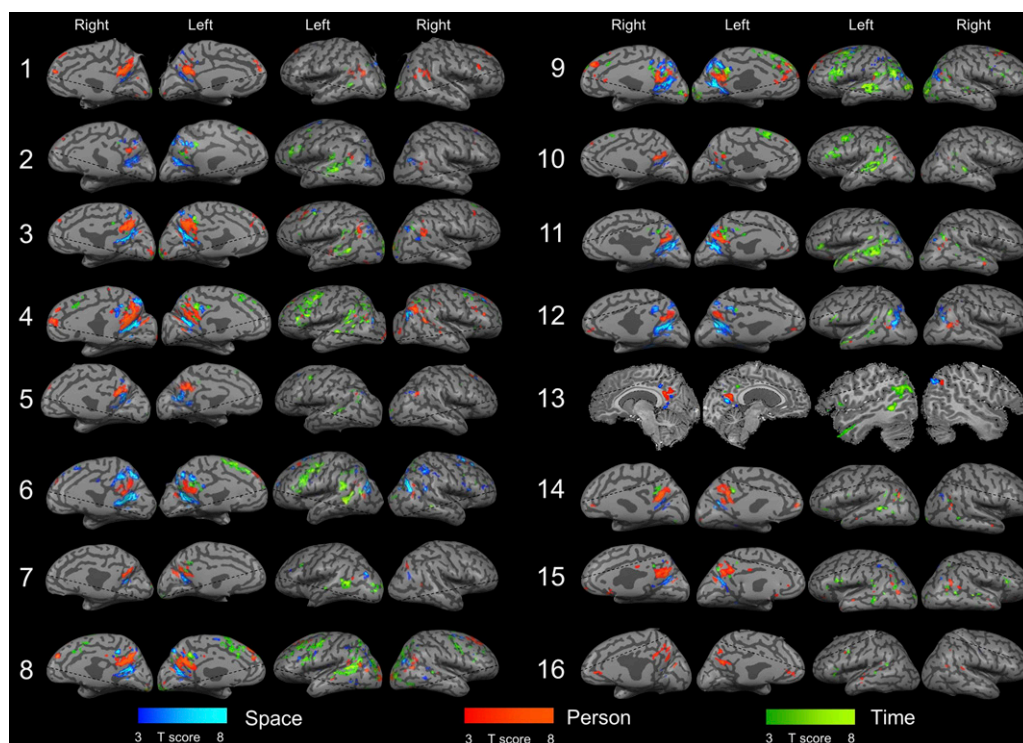
(Figs. 1 and 2 and Fig. S1). Gaps were averaged across subjects between each pair of orientation domains in each region (Table S2). *Measuring the effect of emotional valence, distance, and stimulus length.* To measure the effect of emotional valence, distance from current location, and stimulus length, we used the data from the post-experiment questionnaires (averaged across the two simultaneously presented stimuli) to create parametrically modulated domain-specific regressors. Specific regressors were separately created for events, indicating whether they happened in the past or will happen in the future. GLM analysis was applied as above with these regressors to evaluate their contribution to the signal. *Measuring the effect of response times on brain activations.* To measure the effect of response times on the data, a new design matrix was created with the addition of a response-time regressor (z-transformed to orthogonalize it from the existing orientation-domains regressors, and convolved with a hemodynamic response function). A region-of-interest GLM was performed with the three orientation domain predictors and the response-time predictor, in each activation cluster identified using the contrasts between orientation domains and other domains, as described in *Functional MRI analysis*.

## SI Results

**Orientation-Related Activations Are Not Confounded by Stimulus Properties or Subjects' Response Time.** To search for contamination of our findings by other cognitive factors, we measured the effect of several potential confounding variables: level of emotional valence, stimuli length, past-versus-future events, and distance of stimuli from the subject's self-location in space, time, or person. In 14 out of our 16 subjects, stimulus length across all orientation domains had no effect (in two subjects, an effect was found, yet it was localized only to occipital regions). Future–past differences did not elicit any significant activations in any subject, corroborating previous findings (20, 21, 54, 56). Emotional valence and distance did not activate any region in the space and time domains. In the person domain, emotional valence activated a region in the precuneus in 3 subjects and deactivated this region in 1 subject. This effect is in-line with previous neuroimaging studies of personal affiliation indicating stronger posterior-cingulate/precuneus responses to more familiar people (28, 77). Stimulus distance activated precuneus voxels in one subject and deactivated it in another, again in the person domain only. These analyses demonstrate that the consistent and widespread domain-specific brain activity reported in the previous sections cannot be attributed to these confounding factors.

Analysis of behavioral results indicated that response times in the time domain were significantly higher than in the space and person domains, respectively (means ± SEM; time −1.79 ± 0.03 s; space, −1.55 + 0.03 s; person, −1.51 ± 0.04 s; $F_{(2,45)} = 13.5$, one-way ANOVA; $P < 0.01$, Tukey–Kramer test). This result is in-line with the above-mentioned clinical observations showing that time orientation is the first to be damaged in disorders of orientation such as Alzheimer's disease and is the last to be regained during recovery from disorientation (2, 41, 42). Response times did not contribute to the domain specificity of the activation clusters, as indicated by addition of a response-time regressor to a region-of-interest GLM analysis (Table S1).



**Fig. S1.** Cortical activity during orientation in space, time, and person in individual subjects. Domain-specific activity is shown for all 16 subjects, obtained by contrasting activity between each orientation domain and the other two domains ($P < 0.05$, FDR-corrected, cluster size >20 voxels). Dashed lines represent the limit of the scanned region in each subject. Subject 13 could not be transformed to an inflated brain representation due to technical reasons and is therefore presented by representative slices. Notice the consistent pattern of activity in the inferior parietal, medial parietal, frontal and temporal cortices.

**Fig. S2.** Overlap between activations in the different orientation domains in individual subjects. Overlapping and nonoverlapping activity is shown for all 16 subjects, obtained by contrasting activity between each orientation domain (space, time, and person) and a lexical control task ($P < 0.05$, FDR-corrected, cluster size >20 voxels). Significant overlap was found in 14/16 subjects. Subject 13 could not be transformed to an inflated brain representation due to technical reasons.

**Fig. S3.** Random-effects group analysis. All 16 subjects were analyzed with a random-effects group analysis. (*A*) Contrast between each orientation domain (space, time, or person) and the other two domains, indicating regions of domain-specific activity (*P* < 0.05, FDR-corrected, cluster size >20 voxels). (*B*) Contrast between each orientation domain and the lexical control task (*P* < 0.05, FDR-corrected, cluster size >20 voxels). Dashed lines indicate borders of regions scanned in all 16 subjects, on which the analysis was performed. The Venn diagram (bottom right) demonstrates the prominent overlap between activations in the precuneus and inferior parietal regions.

**Fig. S4.** Probabilistic-maps group analysis. Two groups of subjects were analyzed separately based on the coverage of their functional scans: 10 subjects scanned with frontal and parietal coverage (*Left*), and 6 subjects scanned with temporal and parietal coverage (*Right*). (*A*) Contrast between each orientation domain (space, time, or person) and the other two domains, indicating regions of domain-specific activity. (*B*) Contrast between each orientation domain and the lexical control task. Original maps used for group analysis are presented in Figs. S1 and S2 and are FDR-corrected and cluster size-thresholded at 20 voxels per cluster. The probabilistic maps presented here are thresholded at 25% of subjects of each group.

**Fig. S5.** Overlap between the default-mode network (DMN) and activity during orientation in the person domain for individual subjects. An ICA component clearly corresponding to the DMN could be identified in 13 out of the 16 subjects. A clear overlap is apparent between the DMN and regions of person orientation.



**Fig. S6.** Overlap between the default-mode network (DMN) and activity during orientation in the space domain for individual subjects. Regions of spatial orientation generally lie outside and adjacent to the default-mode network although some overlap exists.

**Fig. S7.** Overlap between the default-mode network (DMN) and activity during orientation in the time domain for individual subjects. Regions of temporal orientation generally lie outside and adjacent to the default-mode network, although some overlap exists. Notice also the strong left-lateralization of time activations.

**Fig. S8.** Average DMN overlap with orientation domains for individual subjects. In each brain region, the average overlap of DMN with each domain-specific region (contrast between each orientation domain and the other two domains) is calculated as the number of DMN voxels in each domain divided by the total number of DMN voxels.

**Fig. S9.** Event-related time courses from default-mode networks nodes, for the different orientation domains. The default-mode network is similarly active across all orientation domains in the precuneus and inferior parietal lobes, and only for the person domain in the medial prefrontal lobe (blue, space; red, person; green, time; error bars represent SEM between subjects).

**Table S1. Response time effect on activity in each orientation-related region**

| Region | Person | Space | Time | Response time (RT) |
|---|---|---|---|---|
| Person-specific regions | | | | |
| Inferior parietal region | **1.55 ± 0.09** | 0.29 ± 0.12 | 0.52 ± 0.08 | 0.08 ± 0.03 |
| Precuneus region | **1.69 ± 0.08** | 0.22 ± 0.08 | 0.24 ± 0.11 | 0.11 ± 0.03 |
| Medial prefrontal region | **1.33 ± 0.14** | −0.29 ± 0.07 | −0.13 ± 0.14 | 0.14 ± 0.04 |
| Lateral temporal region | **1.49 ± 0.19** | 0.13 ± 0.11 | 0.47 ± 0.06 | 0.01 ± 0.07 |
| Space-specific regions | | | | |
| Inferior parietal region | −0.11 ± 0.07 | **1.46 ± 0.06** | 0.41 ± 0.07 | 0.14 ± 0.03 |
| Precuneus region | 0.05 ± 0.05 | **1.60 ± 0.09** | 0.28 ± 0.07 | 0.23 ± 0.04 |
| Time-specific regions | | | | |
| Inferior parietal region | 0.45 ± 0.13 | 0.16 ± 0.11 | **1.57 ± 0.10** | 0.04 ± 0.05 |
| Precuneus region | 0.42 ± 0.10 | −0.09 ± 0.09 | **1.30 ± 0.11** | 0.05 ± 0.02 |
| Medial prefrontal region | 0.64 ± 0.16 | 0.39 ± 0.20 | **1.41 ± 0.13** | 0.11 ± 0.08 |
| Lateral temporal region | 0.18 ± 0.05 | −0.08 ± 0.05 | **1.44 ± 0.06** | 0.06 ± 0.03 |

A region-of-interest GLM was performed on each of the previously identified orientation-specific clusters, with the addition of a response time-specific regressor. The table indicates mean ± SEM of beta values of each regressor, across subjects, in each brain region separately. The domain for which each cluster is specific is highlighted in bold font. As can be observed, response times show a minimal contribution to the variance of each region compared with the main effect of orientation domain.

**Table S2. Gaps between activation clusters in each brain region**

| Contrast | Mean gap ± SEM | | | |
|---|---|---|---|---|
| | Precuneus region | Inferior parietal | Medial prefrontal | Temporal lobe |
| Contrast between each orientation domain and lexical control | | | | |
| Space–person | −37.2 ± 4.0 mm | −25.6 ± 4.5 mm | — | — |
| Person–time | −32.8 ± 5.4 mm | −31.4 ± 5.5 mm | −19.7 ± 12.4 mm | −17.5 ± 8.6 mm |
| Space–time | −31.3 ± 4.3 mm | −32.2 ± 5.0 mm | — | — |
| Contrast between each orientation domain and the other two domains | | | | |
| Space–person | 1.2 ± 0.3 mm | 6.5 ± 1.8 mm | — | — |
| Person–time | 3.9 ± 1.2 mm | 5.7 ± 2.5 mm | 11.4 ± 3.5 mm | 16.7 ± 7.3 mm |
| Space–time | 2.1 ± 0.7 mm | 5.0 ± 2.0 mm | — | — |

Gaps were computed as the minimal Euclidean distance between the borders of each pair of clusters, in each hemisphere separately. In the case of overlapping activity, overlap extent (maximal Euclidean distance between activation borders inside the overlapping region) was represented by a negative value. Numbers represent mean gap and SEM between subjects. Since space-orientation activations do not appear in the medial prefrontal and temporal lobe, comparisons between space and other domains were not computed at these regions (marked with dashes). Activation clusters were taken from results of the contrast between each domain and the lexical control (Fig. 3 and Fig. S3) and the contrast between each domain and the other two domains (Figs. 1 and 2 and Fig. S1). Note that the contrast between domains and lexical control enables measurement of the full extent of activation.